

## Magnon heat conduction and magnon lifetimes in the metallic ferromagnet $\text{Fe}_{68}\text{Co}_{32}$ at low temperatures\*

Y. Hsu and L. Berger

Physics Department, Carnegie-Mellon University, Pittsburgh, Pennsylvania 15213

(Received 17 February 1976)

The thermal and electrical conductivities of the alloy  $\text{Fe}_{68}\text{Co}_{32}$  have been measured with high accuracy between 1.2 and 4.5 K, in external fields up to 5.2 T. The results show that magnons contribute about 10% of the total heat conduction at 4 K. The magnon contribution  $\kappa_m$  varies roughly like  $T^{1.3}$  implying for the magnon lifetime  $\tau_m \propto T^{-1.2} \propto \omega^{-1.2}$ . This is not far from the prediction  $\tau_m \propto \omega^{-1}$  of the  $s$ - $d$  exchange theory of magnon-electron scattering, in the dirty limit  $\Lambda_e q \ll 1$  where  $\Lambda_e$  is the electronic mean free path and  $q$  is the magnon wave number. The magnon lifetime value is  $\tau_m \simeq 7 \times 10^{-10}$  sec at 4 K, which is four times as large as for the nickel-rich Ni-Fe alloys investigated before. This large  $\tau_m$  value is probably caused by the very small electronic density of states at the Fermi level. The effect of dipole-dipole interaction on the magnon dispersion curve is unusually important in  $\text{Fe}_{68}\text{Co}_{32}$ , and is taken into account exactly.

### I. INTRODUCTION

Heat transport by magnons was observed recently<sup>1</sup> in two nickel-rich Ni-Fe alloys, between 1.2 and 4.5 K. This was the first such observation in transition metals. In order to separate this magnon contribution, we used an external magnetic field: the field removes the magnon contribution, while the electron and phonon contributions are field independent above saturation. The results were roughly consistent with a simple kinetic theory of magnon thermal conduction and with the assumption that magnons are scattered by conduction electrons through the so-called  $s$ - $d$  exchange interaction. Magnon lifetime was about  $1.5 \times 10^{-10}$  sec at 4 K, and varied roughly like  $T^{-0.6}$  and  $T^{-1}$  respectively, in the two alloys. The magnon contribution amounted to about 3% of the total thermal conductivity at 4 K.

In a search for materials where the magnon contribution might be larger and easier to measure, we chose the alloy  $\text{Fe}_{68}\text{Co}_{32}$ , which has a saturation magnetization reaching 2.62 T. This alloy corresponds to the highest point of the Slater-Pauling curve. Its electronic structure is rather unusual.<sup>2</sup> The Fermi level for spin up lies above the top of the  $3d$  band while the Fermi level for spin down lies in a gap between two subbands. As a result, its electronic density of states is less than one-half of that of Ni-Fe and Ni-Cu. This should increase considerably the magnon lifetime for any kind of magnon-electron scattering process. Finally, magnon relaxation processes involving spin-orbit interaction would be expected to be less active in iron alloys than in nickel alloys, judging from  $g$ -factor values. Indeed, we find the magnon lifetime in  $\text{Fe}_{68}\text{Co}_{32}$  to be four times as large as in

nickel-rich Ni-Fe alloys, and at least 35 times as large as in our Ni-Cu. The magnon contribution is about 10% of the total conductivity at 4 K.

### II. KINETIC MODELS FOR MAGNON THERMAL CONDUCTIVITY

The thermal conductivity of a magnon gas along the  $z$  axis is given by

$$\kappa_m = \sum c v_z^2 \tau_m, \quad (1)$$

where  $c$  is the specific heat,  $\vec{v}$  the group velocity, and  $\tau_m$  the lifetime of a magnon mode. The dipole-dipole interaction changes<sup>3</sup> the dispersion relation of a magnon, and therefore influences  $c$  and  $\vec{v}$ . This influence was taken into account only to first order in the saturation magnetization  $M_s$  in our work<sup>1</sup> on Ni-Fe. Due to the larger  $M_s$  of Fe-Co, it is advisable to treat the dipole-dipole interaction exactly. The energy of a magnon of wave vector  $\vec{q}$  is<sup>3</sup>

$$\hbar\omega = E(\vec{q}) = \{[E^0(q)]^2 + g\mu_B M_s \sin^2\theta E^0(q)\}^{1/2}, \quad (2)$$

where

$$E^0(q) = Dq^2 + g\mu_B B_E,$$

and where  $B_E$  is the external field,  $\theta$  is the angle between  $\vec{q}$  and  $\vec{M}_s$ , and the mks system is used everywhere. We assume  $\vec{M}_s$ ,  $\vec{B}_E$ , and the heat flow all to be parallel to the  $z$  axis, and we define

$$\begin{aligned} x &= Dq^2/k_B T, \quad z = g\mu_B B_E/k_B T; \\ j &= g\mu_B M_s/k_B T, \quad a = \cos\theta; \\ l &= E(\vec{q})/k_B T = [(x+z)^2 + j(x+z)(1-a^2)]^{1/2}. \end{aligned} \quad (3)$$

Combining Eqs. (1)–(3), we obtain

$$\kappa_m = \frac{k_B^{7/2} T^{5/2}}{\hbar^2 D^{1/2} 8\pi^2} \int_{x=0}^{+\infty} \int_{a=-1}^{+1} \tau_m \frac{e^x}{(e^x - 1)^2} \times [2(x+z)x - jz(1-a^2)]^2 \times a^2 da \frac{dx}{x^{1/2}}. \quad (4)$$

If magnon-electron scattering mediated by the  $s$ - $d$  exchange interaction is assumed to be dominant, and if the "dirty" limit  $\Lambda_e q \ll 1$  holds, where  $\Lambda_e$  is the electron mean free path, then one can show<sup>1,4</sup> that  $\tau_m \propto \omega^{-1}$ , or  $\tau_m = 1/2\alpha\omega$ , where  $\alpha$  is the so-called Gilbert parameter. Then Eq. (4) becomes

$$\kappa_m(M_s, B_E, T) = \frac{k_B^{5/2} T^{3/2}}{16\pi^2 \hbar D^{1/2} \alpha} J_D(j, z),$$

$$J_D(j, z) = \int_{x=0}^{\infty} \int_{a=-1}^1 \frac{e^x}{l(e^x - 1)^2} \times [2(x+z)x - jz(1-a^2)]^2 a^2 da \frac{dx}{x^{1/2}}. \quad (5)$$

For  $B_E = M_s = 0$ ,  $J_D(0, 0) = \frac{8}{3}\Gamma(\frac{7}{2})\zeta(\frac{5}{2}) = 11.883$ , and  $\kappa_m \propto T^{1.5}$ . Also, the integrand  $x^{5/2}e^x/(e^x - 1)^2$  in the integral  $J_D(0, 0)$  has a peak at  $x = 1.8$ . The different assumptions,<sup>1</sup>  $\tau_m = \text{const}$  and  $\tau_m \propto \omega^{-1/2}$  would have put the peak respectively at  $x = 3.2$  and  $x = 2.6$  instead. The integral  $J_D$  has been evaluated for various values of  $z$  and  $j$ , with the help of a digital computer (Fig. 1).

By examining carefully the curves of Fig. 1, we have found the following approximate relation to hold

$$J_D(j, z) \approx J_D(0, z_{\text{eff}}),$$

$$z_{\text{eff}} = z + f(j). \quad (6)$$

The function  $f(j)$  is shown as a solid curve in the insert of Fig. 1. In the same insert, the dashed line represents the "effective-field" approximation  $f(j) = \frac{7}{15}j$  or  $B_{\text{eff}} = B_E + \frac{7}{15}M_s$  described in the Appendix of Ref. 1, which is correct only to first order in  $j$  or  $M_s$ . While  $z_{\text{eff}}$  can always be defined, a temperature-independent effective field  $B_{\text{eff}}$  can be defined only if  $j < 1$ . For  $\text{Fe}_{68}\text{Co}_{32}$  at  $1.5 < T < 4.5$  K, we have  $2.5 > j > 0.8$ . In Ref. 1, we erroneously stated the expansion parameter to be  $M_s/B_E$  rather than  $j$ .

In the "clean" (or "anomalous") limit  $\Lambda_e q \gg 1$ , not only energy conservation but also momentum conservation plays a role in restricting possible nonflip magnon-electron collisions. As a result, we have now<sup>5</sup>  $1/\tau_m = b\omega/q$ , where  $b$  is a constant.

Therefore Eq. (4) becomes

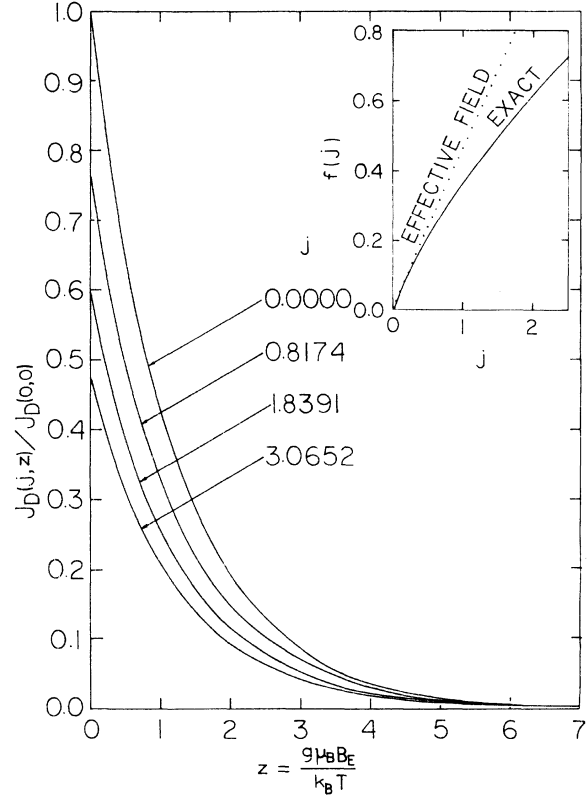


FIG. 1. Predicted magnon thermal conductivity at a field  $B_E = 0$ , normalized to the conductivity at  $B_E = 0$ , in the dirty limit. The insert shows the function  $f(j)$  appearing in the quantity  $z_{\text{eff}} = z + f(j)$ , which describes the effect of dipole-dipole interaction.

$$\kappa_m(M_s, B_E, T) = \frac{k_B^3 T^2}{8\pi^2 \hbar b D} J_C(j, z),$$

$$J_C(j, z) = \int_{x=0}^{\infty} \int_{a=-1}^1 \frac{e^x}{l(e^x - 1)^2} \times [2(x+z)x - jz(1-a^2)]^2 a^2 da dx. \quad (7)$$

For  $B_E = M_s = 0$ ,  $J_C(0, 0) = \frac{8}{3}\Gamma(4)\zeta(3) = 19.232$  and  $\tau_m \propto \omega^{-1/2}$ ,  $\kappa_m \propto T^2$ . In Ref. 1, we assumed  $\tau_m \propto \omega^{-1/2}$  even at  $B_E \neq 0$ , which is not quite correct. The integrand  $x^3 e^x/(e^x - 1)^2$  in the integral  $J_C(0, 0)$  has a peak at  $x = 2.6$ . The integral  $J_C(j, z)$  has been evaluated with the help of a computer.

Using Eqs. (5) or (7), the variation of the magnon thermal conductivity between two field values,  $B_{E1}$  and  $B_{E2}$ , can be written

$$\frac{\kappa_m(M_s, B_{E2}, T) - \kappa_m(M_s, B_{E1}, T)}{\kappa_m(0, 0, T)} = \frac{J(j, z_2) - J(j, z_1)}{J(0, 0)}, \quad (8)$$

where  $J$  may be  $J_D$  or  $J_C$ , depending on conditions.

Actually, the choice between  $J_D$  and  $J_C$  affects

the right-hand side of Eq. (8) only by a few percent. If we substitute experimental values of  $[\kappa_m(M_s, B_E, T) - \kappa_m(M_s, B_{E1}, T)]$  into Eq. (8), we can solve for the values of  $\kappa_m(0, 0, T)$ .

### III. SAMPLE PREPARATION

The sample was prepared from high-purity Johnson-Matthey metals by levitation induction melting in an atmosphere of helium and cast into an alumina mold. It was hot rolled in air through a small rolling mill at about 800 °C, and machined to the final shape  $0.47 \times 0.50 \times 6.5$  cm<sup>3</sup>. Then it was homogenized for 48 h at 1385 °C in a slow flow of hydrogen dried and purified by passing through a liquid-nitrogen trap. The temperature was then lowered to 900 °C, and the sample was annealed in a vacuum of about  $1 \times 10^{-5}$  Torr for 2 h in order to remove any dissolved hydrogen. Finally, it was furnace cooled.

The sample has grains of about 0.5–1 cm in diameter. Wet chemical analysis gave 33.5-wt% Co, which corresponds to the atomic composition  $\text{Fe}_{68}\text{Co}_{32}$ .

### IV. EXPERIMENTAL APPARATUS

The apparatus used in thermal conductivity measurements is an improved version of the one described in Ref. 1. In order to optimize the thermal grounding of electrical leads going to the sample, they now pass through the liquid-helium bath, and enter the vacuum can through a feedthrough made of Stycast 2850 low-expansion epoxy resin.<sup>6</sup> The radiation baffle in the vacuum line has been made more effective. Because of the larger saturation magnetization of iron alloys, it is advisable to reduce the demagnetizing factor by using a longer and thinner sample. It is then possible to wind the heaters  $H_1$  and  $H_2$  directly around the sample.

The two Allen-Bradley  $\frac{1}{8}$ -W 100- $\Omega$  carbon resistors  $R_1$  and  $R_2$  are connected to the arms of a new type<sup>7</sup> of ac bridge which allows to measure directly  $R_1$  and  $R_1 - R_2$  on separate decades while still eliminating the influence of lead resistance. The method of calibration of  $R_1$  and  $R_2$  is the same as in Ref. 1. The unexplained  $\lambda$ -point discontinuities mentioned in Ref. 1 are now somewhat smaller. This may be due to the fact that we now regulate the bath pressure with a rubber-diaphragm mechanical manostat,<sup>8</sup> thus removing the heating of the bath caused by our earlier electronic regulator.

Although the systematic deviations between the actual values of  $R_1(T)$  or  $R_2(T)$  and the values given by the fitted Clement-Quinnell analytical expression<sup>1</sup> are small, it is essential to take them into account; we perform the “zeroth-law test,” by

checking that the temperatures  $T_1$  and  $T_2$  calculated by the analytical expression from  $R_1$  and  $R_2$  values measured under zero heater power are exactly equal. A small additive correction to  $T_1$  is made if they are not equal.

The power in heater  $H_1$  is chosen in such a way that  $(T_1 - T_2)/T_2 \approx 2\%$ . The method used to measure the electrical resistance of the sample is the same as in Ref. 1.

### V. EXPERIMENTAL RESULTS

The electrical resistivity in zero field is  $9.49 \times 10^{-8}$   $\Omega$  m at room temperature and  $5.42 \times 10^{-8}$   $\Omega$  m at 4.2 K. In longitudinal fields, it increases by about 1.5% up to saturation at 4.2 K. Above saturation, it increases very slowly, being given by  $\rho_{\parallel} = 5.503 + 0.00476 B_E$ , where  $\rho_{\parallel}$  is given in units of  $10^{-8}$   $\Omega$  m and  $B_E$  in tesla. It was measured up to 5.3 T, at temperatures of 4.2 and 1.9 K. To the experimental accuracy of  $\pm 0.1\%$ , it was the same at the two temperatures, showing that the alloy is in the residual resistance region where electron scattering is mostly elastic. Therefore, we can use the theoretical Fermi-Dirac value  $L_{\text{th}} = 2.44 \times 10^{-8}$  V<sup>2</sup>/K<sup>2</sup> of the Lorenz number, in order to calculate the electronic part  $\kappa_e$  of the thermal conductivity by the Wiedemann-Franz law  $\kappa_e = L_{\text{th}} T / \rho_{\parallel}$  (Fig. 2). The small variation  $\Delta\kappa_e$  between two fields at a given temperature can be calculated similarly (Table I, third column).

The thermal conductivity was measured at fields of 0, 0.669, 2.930, and 5.192 T, all parallel to the heat current (Fig. 2). The last three field values are sufficient to saturate the sample. Three runs were made at the second and third field values. Six runs were made at the highest field, because the dispersion of data points was the largest at that field. For clarity, only one run is shown for each field on Fig. 2. Data dispersion is usually about  $\pm 0.3\%$ . The total conductivity  $\kappa$  is seen to decrease for increasing fields, above saturation. The  $\kappa$  data are fitted at each field to third-order polynomials, shown as solid curves in Fig. 2. Using these smooth curves, we can evaluate the variation of conductivity  $\Delta\kappa$  between the two field values 0.669 and 5.192 T (second column of Table I). Then assuming  $\Delta\kappa = \Delta\kappa_e + \Delta\kappa_m$ , we find  $\Delta\kappa_m$  (Table I, fourth column). Substituting it into the numerator on the left-hand side of Eq. (8), we derive the magnon conductivity  $\kappa_m(0, 0, T)$  given in the fifth column of Table I and in Fig. 3. We assume the dirty limit to apply, and use  $J_D(j, z)$  in Eq. (8). We take  $M_s = 2.62$  T (Ref. 9),  $g = 2.09$  (Ref. 10),  $D = 6.84 \times 10^{-40}$  J m<sup>2</sup> (Ref. 11).

As a check, we can use these values of  $\kappa_m$  and Eq. (8) to predict the variation  $\Delta\kappa$  between 0.669 T

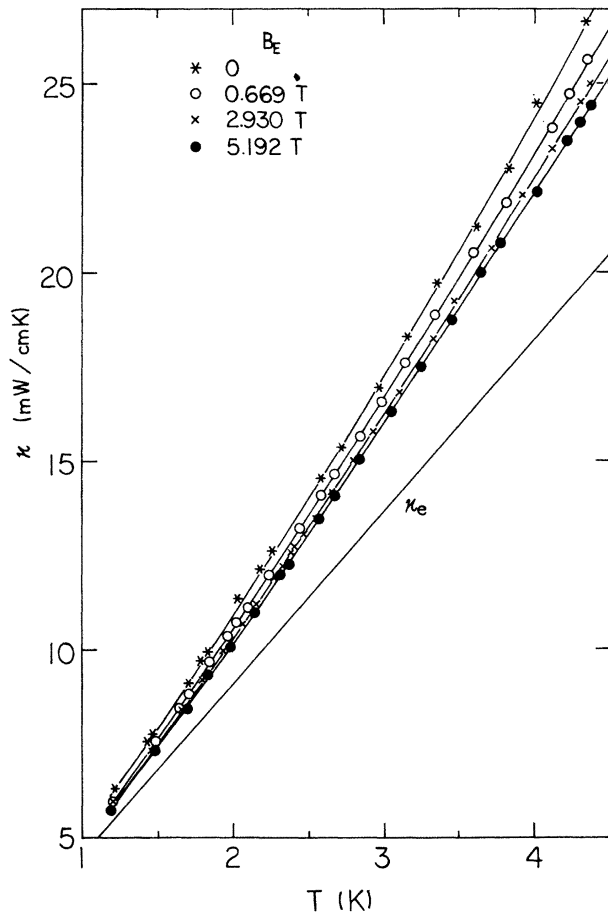


FIG. 2. Measured thermal conductivity  $\kappa$  at various fields, and calculated electronic thermal conductivity  $\kappa_e$  at saturation.

and the middle-field value 2.930 T. This predicted  $\Delta\kappa$  is found to agree well with the directly measured  $\Delta\kappa$  between the same field values.

Substituting our  $\kappa_m(0, 0, T)$  values into Eq. (5), we can solve for  $\alpha$  at any given temperature (Table I). Then we define an average magnon

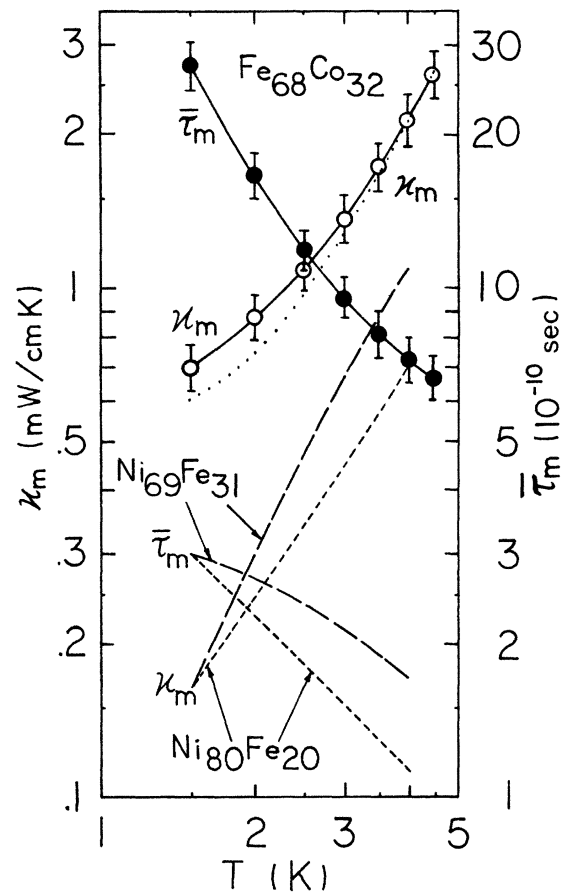


FIG. 3. Magnon thermal conductivity  $\kappa_m$  of  $\text{Fe}_{68}\text{Co}_{32}$  at  $B_E = M_S = 0$ , and magnon lifetime  $\bar{\tau}_m$ . The dotted line shows the  $\kappa_m$  values as calculated with the effective-field approximation. The curves for Ni-Fe alloys are from Ref. 1.

lifetime  $\bar{\tau}_m = 1/2\alpha\bar{\omega}$ , where we choose  $\bar{\omega} = 1.8k_B T/\hbar$  for the average magnon frequency since the integrand in  $J_D(0, 0)$  peaks at  $x = 1.8$ . The resulting values of  $\bar{\tau}_m$  are shown in Table I and Fig. 3.

We have also calculated  $\bar{\tau}_m$  by the effective-field

TABLE I. Experimental quantities for  $\text{Fe}_{69}\text{Co}_{32}$ . The fifth column shows the magnon thermal conductivity. The sixth column shows the Gilbert parameter of thermal magnons. The seventh and eighth columns show their frequency and lifetime. Data analysis is based on the dirty limit.

$T$ (K)	$\Delta\kappa$ (mW/cm K)	$\Delta\kappa_e$ (mW/cm K)	$\Delta\kappa_m$ (mW/cm K)	$\kappa_m$ (mW/cm K)	$\alpha$ ( $10^{-3}$ )	$\bar{f} = \bar{\omega}/2\pi$ (GHz)	$\bar{\tau}_m$ ( $10^{-10}$ sec)
1.5	-0.2267	-0.0202	-0.2091	0.6967	0.51	56.4	27.46
2.0	-0.3438	-0.0269	-0.3089	0.8635	0.63	75.2	16.58
2.5	-0.4760	-0.0337	-0.4423	1.0901	0.70	94	11.98
3.0	-0.6265	-0.0404	-0.5861	1.3764	0.73	113	9.59
3.5	-0.7958	-0.0471	-0.7487	1.7255	0.73	132	8.18
4.0	-0.9844	-0.0539	-0.9306	2.1420	0.72	150	7.27
4.5	-1.1928	-0.0606	-1.1322	2.6311	0.70	169	6.65

approximation (see Sec. II and Ref. 1), and the results are shown as the dotted line in Fig. 3. The relative error introduced by this approximation is the largest at the lowest temperatures. Even in the case of a high-magnetization material such as ours, this error does not exceed 15%.

If we consider the actual Lorenz number  $L = \kappa \rho_{\parallel} / T$  of our alloy, our data at 4 K yield  $L/L_{\text{th}} = 1.3$ .

## VI. DISCUSSION OF RESULTS

Our results show that magnons contribute about 10% of the heat conduction at 4 K. Figure 3 shows that  $\kappa_m(0, 0, T)$  varies like  $T^{1.3}$  on the average over the range 1.5–4.5 K. This is close to the  $T^{1.5}$  variation predicted by Eq. (5) for the dirty limit. The agreement is even better if we consider only the data between 2 and 4.5 K, where  $\kappa_m \propto T^{1.5}$  on the average (Fig. 3). Correspondingly, we find  $\bar{\tau}_m \propto T^{-1.2} \propto (\bar{\omega})^{-1.2}$  on the average between 1.5 and 4.5 K, in approximate agreement with the  $T^{-1} \propto (\bar{\omega})^{-1}$  prediction of the *s-d* exchange model in the dirty limit. And we find exactly  $\bar{\tau}_m \propto T^{-1} \propto (\bar{\omega})^{-1}$  between 2 and 4.5 K. Our Fe-Co results are an *a posteriori* justification of the choice of the dirty limit and of Eq. (5) to analyze our data. We have also tried to use the clean limit [Eq. (7)], but self-consistency is not obtained in that case. At 4 K,  $\bar{\tau}_m = 7.3 \times 10^{-10}$  sec, which is at least four times the values found in nickel-rich Ni-Fe alloys.<sup>1</sup> For comparison, these earlier Ni-Fe results are included in Fig. 3. Note that the  $\bar{\tau}_m$  and  $\bar{\omega}$  values are affected by the slightly different mathematics used in Ref. 1.

As we noted in Sec. I, these large magnon lifetimes in  $\text{Fe}_{68}\text{Co}_{32}$  may be related to the unusually small electronic density of states at the Fermi level.

Also, electron-magnon collisions involving spin-orbit interaction (i.e., anisotropic *s-d* exchange) would be expected to be less active in Fe-rich alloys than in Ni or Ni-Cu, judging from the smaller values of  $|g-2|$ , and from the scarcity of or-

bit degeneracies. This is experimentally confirmed too,<sup>12</sup> since  $\alpha \approx 25 \times 10^{-3}$  for Ni at 300 K, and  $\alpha \approx 2.2 \times 10^{-3}$  only for Fe at 300 K, from ferromagnetic resonance data.

It is interesting that such a long magnon lifetime is achieved in a highly magnetostrictive material like  $\text{Fe}_{68}\text{Co}_{32}$ . This shows that magnon-phonon scattering is not a significant process for magnon relaxation in metals.

We chose the Gilbert<sup>13</sup> parameter  $\alpha = 1/2\omega\tau_m$  in order to describe spin-wave relaxation, because it has the advantage of being dimensionless, and of having a simple meaning related to the inverse of the quality factor (*Q* factor) of a spin-wave mode. The factor 2 in the denominator of this equation comes from fact that  $\tau_m$  describes the relaxation of  $M_z$  while  $\alpha$  describes the relaxation of  $M_x$  and  $M_y$ . The Landau-Lifshitz parameter  $\lambda = \gamma M_s \alpha$ , where  $\gamma = g\mu_B/\hbar$ , is more commonly used. For  $\text{Fe}_{68}\text{Co}_{32}$  at 1–4 K, we find  $\alpha \approx 0.71 \times 10^{-3}$ , or  $\lambda \approx 3.4 \times 10^8$  sec<sup>-1</sup> in mks units. If cgs units are used, this becomes  $\lambda_{\text{cgs}} = \lambda/4\pi = 0.27 \times 10^8$  sec<sup>-1</sup>.

## VII. DIRECT EVALUATION OF $\Lambda_e q$

Using existing data<sup>14</sup> for the ordinary Hall constant  $R_0$  and our measured value for the resistivity  $\rho$ , we can derive a rough value of  $\Lambda_e$ . Assuming a spherical Fermi surface, we obtain  $\Lambda_e = 3.45 \times 10^{-8}$  m. From the known value<sup>11</sup> of  $D$  and from the average spin-wave energy  $1.8k_B T$ , we also find  $q$ . Finally, this yields  $\Lambda_e q = 7.9$  at 1.5 K and  $\Lambda_e q = 13.8$  at 4.5 K.

It is interesting, though disturbing, that these values suggest the clean rather than the dirty limit. However,  $R_0$  and  $\rho$  are determined mainly by some electrons of high mobility and strong *4s* character. In the case of *3d* electrons of low mobility and short  $\Lambda_e$ ,  $\Lambda_e q$  may be smaller by one order of magnitude and approach the dirty limit. This removes the contradiction.

\*Work supported by the U. S. NSF.

<sup>1</sup>W. B. Yelon and L. Berger, Phys. Rev. B **6**, 1974 (1972).

<sup>2</sup>L. Berger, Phys. Rev. **137**, A220 (1965).

<sup>3</sup>T. Holstein and H. Primakoff, Phys. Rev. **58**, 1098 (1940).

<sup>4</sup>R. E. Prange and V. Korenman, J. Magn. Res. **6**, 274 (1972); V. Korenman and R. E. Prange, Phys. Rev. B **6**, 2769 (1972); V. Kambersky, Can. J. Phys. **48**, 2906 (1970).

<sup>5</sup>E. A. Turov, Bull. Acad. Sci. USSR, Phys. Ser. **19**, 414 (1955); A. H. Mitchell, Phys. Rev. **105**, 1439 (1957); S. V. Vonsovskii and Yu. A. Izyumov, Phys. Metals Metallogr. (USSR) **10**, 1 (1960).

<sup>6</sup>A. C. Anderson, Rev. Sci. Instrum. **39**, 605 (1968).

<sup>7</sup>Y. Hsu, Rev. Sci. Instrum. **46**, 1109 (1975).

<sup>8</sup>M. M. Kreitman, Rev. Sci. Instrum. **35**, 749 (1964).

<sup>9</sup>R. M. Bozorth, *Ferromagnetism* (Van Nostrand, New York, 1951), p. 194.

<sup>10</sup>G. G. Scott and H. W. Sturmer, Phys. Rev. **184**, 490 (1969).

<sup>11</sup>R. D. Lowde, M. Shimizu, M. W. Stringfellow, and B. H. Torrie, Phys. Rev. Lett. **14**, 698 (1965).

<sup>12</sup>S. M. Bhagat and P. Lubitz, Phys. Rev. B **10**, 179 (1974). See their Fig. 7.

<sup>13</sup>See, for the definition of  $\alpha$  and  $\lambda$ , S. Iida, J. Phys. Chem. Solids **24**, 625 (1963).

<sup>14</sup>F. P. Beitel and E. M. Pugh, Phys. Rev. **112**, 1516 (1958).